ORIGINAL PAPER

A comparative theoretical study for the methanol dehydrogenation to CO over Pt_3 and $PtAu_2$ clusters

Wenhui Zhong · Yuxia Liu · Dongju Zhang

Abstract The density functional theory (DFT) calculations are carried out to study the mechanism details and the ensemble effect of methanol dehydrogenation over Pt_3 and $PtAu_2$ clusters, which present the smallest models of pure Pt clusters and bimetallic PtAu clusters. The energy diagrams are drawn out along both the initial O-H and C-H bond scission pathways via the four sequential dehydrogenation processes, respectively, i.e., $CH_3OH \rightarrow CH_2OH \rightarrow CH_2O \rightarrow CHO \rightarrow CO$ and $CH_3OH \rightarrow CH_3O \rightarrow CH_2O \rightarrow CHO \rightarrow CO$, respectively. It is revealed that the reaction kinetics over $PtAu_2$ is significantly different from that over Pt_3. For the Pt_3-mediated reaction, the C-H bond scission pathway, where an ensemble composed of two Pt atoms is required to complete methanol dehydrogenation, is energetically more favorable than the O-H bond scission pathway, and the maximum barrier along this pathway is calculated to be 12.99 kcal mol^{-1}. In contrast, $PtAu_2$ cluster facilitates the reaction starting from the O-H bond scission, where the Pt atom acts as the active center throughout each elementary step of methanol dehydrogenation, and the initial O-H bond scission with a barrier of 21.42 kcal mol^{-1} is the bottomneck step of methanol decomposition. Importantly, it is shown that the complete dehydrogenation product of methanol, CO, can more easily dissociate from $PtAu_2$ cluster than from Pt_3 cluster. The calculated results over the model clusters provide assistance to some extent for understanding the improved catalytic activity of bimetal PtAu catalysts toward methanol oxidation in comparison with pure Pt catalysts.

W. Zhong · Y. Liu · D. Zhang (✉)
Key Lab of Colloid and Interface Chemistry,
Ministry of Education, Institute of Theoretical Chemistry,
Shandong University,
Jinan 250100, People's Republic of China
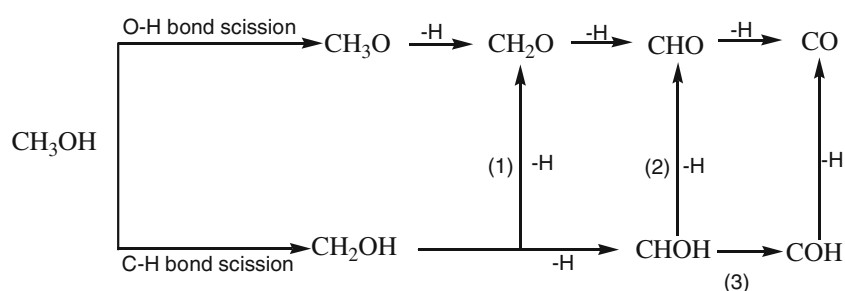e-mail: zhangdj@sdu.edu.cn

Introduction

Methanol is considered as one of the most important candidates for storage and production of hydrogen and is a promising compound in the next generation of renewable green fuels [1]. Pt-based catalysts are known to possess excellent catalytic activity for methanol oxidation [2–7]. However, it is well-known that pure Pt catalysts used in direct-methanol fuel cells (DMFCs) are easily poisoned by the carbonyl species generated in the electrochemical oxidation of methanol [8]. The use of bimetallic catalysts is indicated to be one of the solutions to reduce CO poisoning and improve the catalyst performance [9–11]. Many Pt-based bimetallic catalysts, such as PtRu [2–4], PtAu [5–7], PtCo [12], PtMo [13], and PtSn [14, 15], have been found to have higher activity for the methanol dehydrogenation reaction with improved resistance to CO poisoning than pure Pt catalysts, and have been applied successfully to prototypes of commercial DMFCs. In particular, PtAu bimetallic nanoparticles, which have attracted much attention over the past twenty years [16, 17], have been proposed as excellent electrocatalysts for methanol electrooxidation [5, 18–23] because Au is more stable than non-noble metals under the DMFCs operating conditions and relatively less expensive than other noble metal materials.

A number of elegant experimental studies have contributed to understanding the intrinsic mechanism of methanol oxidation over Pt-based catalysts [24–35]. As is shown in Scheme 1, researchers have proposed two general reaction pathways: one starts from the O-H bond scission [36], and the other arises from the breaking of C-H bond [37].

Scheme 1 General reaction pathways of the methanol dehydrogenation to CO

$$CH_3OH \xrightarrow{\text{O-H bond scission}} CH_3O \xrightarrow{\text{-H}} CH_2O \xrightarrow{\text{-H}} CHO \xrightarrow{\text{-H}} CO$$

$$CH_3OH \xrightarrow{\text{C-H bond scission}} CH_2OH \xrightarrow{\text{-H}} CHOH \xrightarrow{} COH$$

with vertical steps labeled (1) -H, (2) -H, (3), and -H.

Theoretically, several groups have also investigated the mechanism of methanol decomposition on pure Pt catalysts on atomic and molecular levels [38–40]. However, a general consensus has still not been reached on which pathway is preferred in the methanol dehydrogenation reaction. For example, Greeley and Mavrikakis [38, 39] proposed that the C-H scission pathway on Pt(111) is dominant, whereas Watanabe [40] argues that the O-H scission pathway on Pt surface is energetically favorable. Additionally, there is only limited knowledge about the mechanism details of the methanol dehydrogenation reaction on PtAu bimetallic catalysts [41], which is crucial to understand the improved catalytic activity of the bimetallic catalysts toward methanol oxidation. Furthermore, the ensemble effect that describes the synergistic behavior of PtAu bimetallic catalysts in specific arrangements [42, 43] is not understood yet. For example, Tong et al. [44] proposed that three Pt atoms together on an ensemble are required for methanol electro-oxidation, while Cuesta et al. [45] found that an ensemble with two adjacent Pt atoms exhibits the ability of the methanol oxidation. Theoretically, by performing DFT calculations, Neurock et al. found all ensembles composed of 1–4 Pt atoms can promote methanol oxidation [46], in contrast to the suggestion from Wu [47] that an isolated Pt atom on surface was inactive for methanol dehydrogenation. These inconsistent facts appeal to further studies for the methanol dehydrogenation to CO over Pt-based catalysts. Within this scenario, here we present a comparative theoretical study on the methanol dehydrogenation to CO over pure Pt₃ cluster and bimetallic PtAu₂ cluster at the molecular level. On the basis of the calculated results, we expect to provide a better understanding about the detailed mechanism and the ensemble effect of methanol dehydrogenation on pure Pt catalysts and bimetallic PtAu catalysts.

Models and computational details

It is generally accepted that gas-phase clusters can be used as model systems to shed light on intrinsic mechanisms of nanocatalysis taking place in realistic and complicated catalytic systems [48, 49]. In this work, we mimic the catalysis of pure Pt catalysts and bimetallic PtAu catalysts for the

methanol dehydrogenation using the simplest Pt₃ and PtAu₂ clusters. Given that the ground states of both the clusters are found to be in their singlets, our calculations for the methanol dehydrogenation over Pt₃ and PtAu₂ are carried out on the singlet potential energy surfaces.

The calculations have been performed using the GAUSSIAN 03 code [50]. In the framework of density functional theory (DFT), we employ the hybrid B3LYP [51–53] functional to explore the stationary points on the potential energy surfaces (PESs). Considering the strong relativistic effects of Au and Pt, we used the Los Alamos LANL2DZ effective core pseudopotentials (ECP) and valence double-ζ basis sets [54, 55] for Au and Pt. The C, H, and O atoms were treated with the 6-311+G(d,p) basis set. No symmetric constraints were imposed during geometrical optimizations. Optimized minima and transition states have been confirmed by performing analytical vibration frequency calculations. Intrinsic reaction coordinates (IRC) [56] calculations have been performed to verify that each saddle point links two desired minima. Stability tests of wave functions for all identified stationary points have been carried out to ensure that the lowest energy solutions in the SCF procedures are found. All calculations are carried out by resolving restricted Kohn-Sham equations [57].

Results and discussion

In order to understand the oxidation mechanism of methanol and to get a complete picture for the methanol dehydrogenation, we examined the reaction pathways along O-H and C-H bond scissions over Pt₃ and PtAu₂ clusters. Optimized structures and calculated energy diagrams are shown in Figs. 1, 2, 3, 4, 5, 6, 7, 8. Note that in this paper, the entropy change in gas phase is much larger than in the solution for the bimolecular reaction, because the translation and rotational movements are suppressed in solution. So in the present work, relative electronic energies are used to analyze the reaction mechanism as done in many excellent publications.

In the following sections, we first describe the mechanism details of methanol oxidation starting from both O-H and C-H bond scissions over Pt₃ cluster, and then discuss

Fig. 1 Potential energy profile of methanol dehydrogenation starting from O–H bond scission over Pt_3 cluster. The energies include zero-point energy corrections
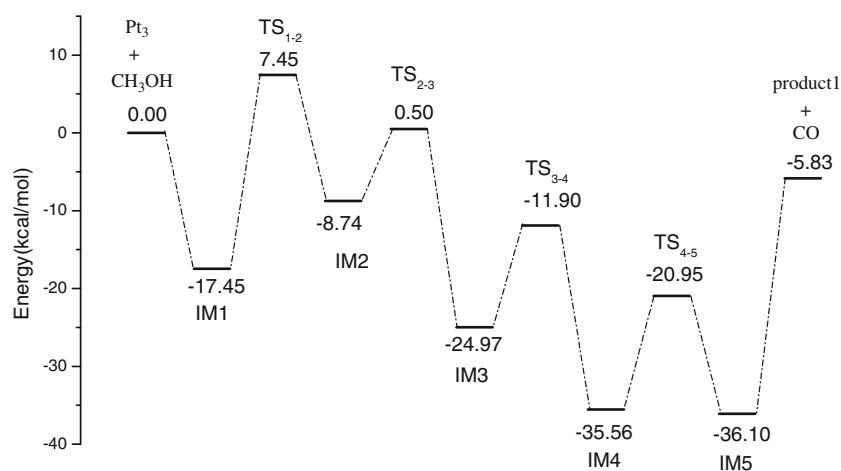
those over $PtAu_2$ cluster. Finally, by comparing the reactivity difference over two clusters, we elucidate the intrinsic reason why bimetallic PtAu nanoparticles exhibit improved catalytic activity toward methanol oxidation.

O-H bond scission branch over Pt_3

Figure 1 shows the calculated potential energy profile for the methanol oxidation over Pt_3 starting from O-H bond scission, and the intermediates and transition states involved along this pathway are given in Fig. 2. The reaction starts

from the binding of methanol molecule to the on-top site of a Pt atom through its O atom, forming intermediate IM1. This scenario is in agreement with the previous works on Pt surface [38, 40]. In IM1, Pt-O distance is calculated to be 2.220 Å, and the binding energy is predicted to be 17.45 kcal mol^{-1}. As shown in Figs. 1, 2, this pathway consists of four sequential dehydrogenation steps, $CH_3OH \rightarrow CH_3O \rightarrow CH_2O \rightarrow CHO \rightarrow CO$, which involves four transition states (TS_{1-2}, TS_{2-3}, TS_{3-4}, and TS_{4-5}) and five intermediates (IM1-IM5). The barriers of four elementary steps are 24.90, 9.24, 13.07, and 14.61 kcal mol^{-1}. Clearly, the initial O-H bond scission is the rate-determining step,

Fig. 2 Optimized geometries of intermediates and transition states involved in the methanol dehydrogenation reaction starting from O–H bond scission over Pt_3 cluster. The blue, gray, red, and white balls denote Pt, C, O and H atoms, respectively. The distances are in Å
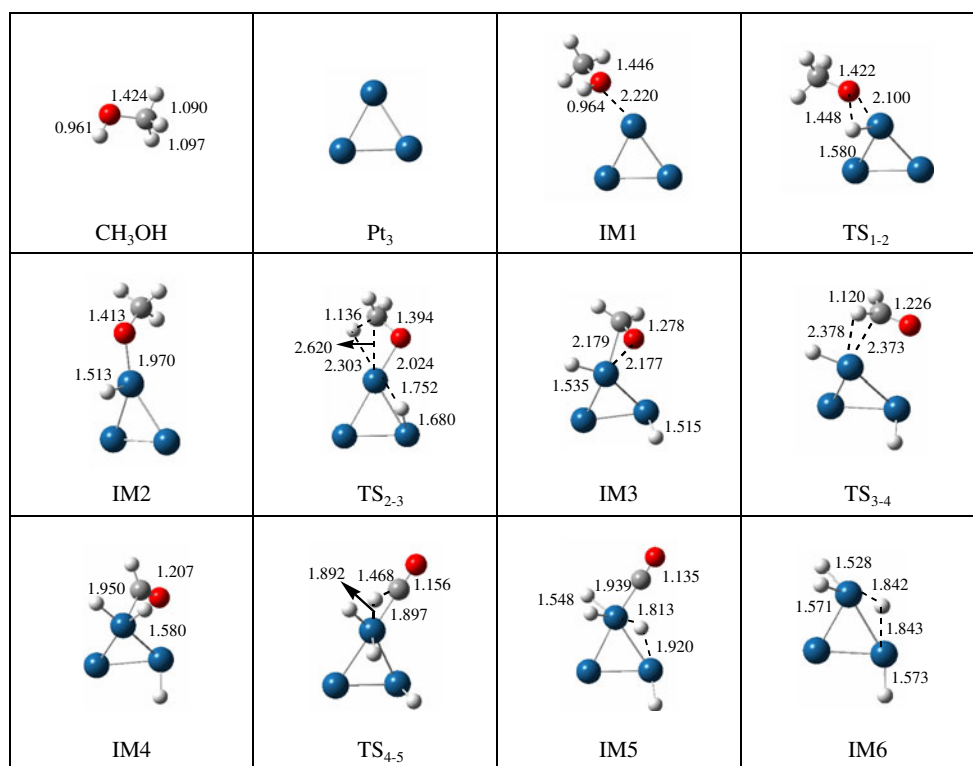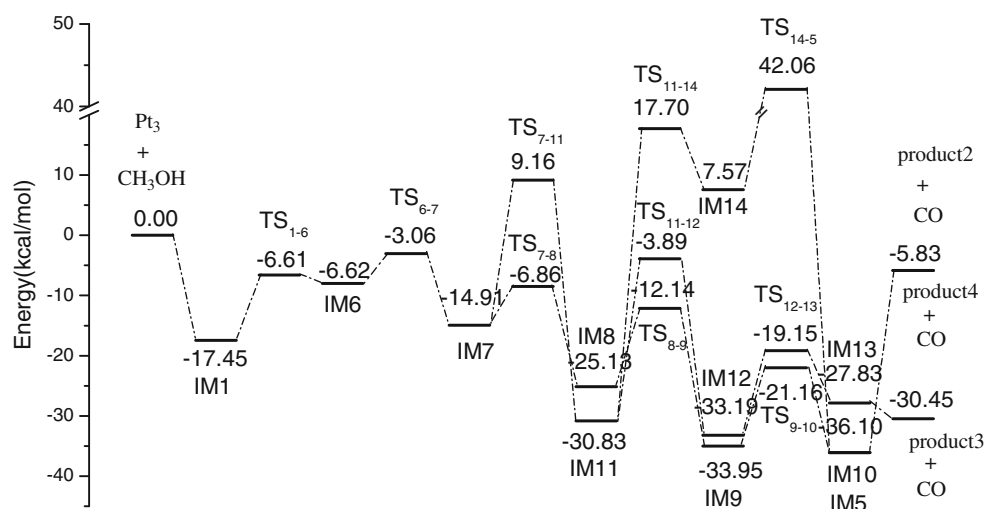
which is endothermic by 8.71 kcal mol⁻¹. After the O-H scission, the following three C-H bond scissions are expected to proceed easily because they are all exothermic processes with low barriers. We notice that IM5 corresponds to the product of complete dehydrogenation of methanol, where all four H atoms in methanol have been transferred to Pt$_3$ cluster and the adsorbed CO is formed.

As is shown in Fig. 2, the O-H activation of methanol, as well as the subsequent three C-H activations, takes place over one Pt atom, implying that the catalytic behavior of small Pt clusters is significantly different from that of Pt surfaces, where an ensemble with 2–4 adjacent Pt atoms was proposed to be necessary to catalyze the reaction [44–46].

C-H bond scission pathway *is located at an on-top site of the cluster*

Figure 3 shows the energy profile calculated along the C-H bond scission pathway, and Fig. 4 collects the optimized geometries of the intermediates and transition states. This pathway is more complex than the O-H bond scission pathway. As shown in Scheme 1, it divides into three branches after the initial C-H bond scission: (I) $CH_3OH \rightarrow CH_2OH \rightarrow CH_2O \rightarrow CHO \rightarrow CO$; (II) $CH_3OH \rightarrow CH_2OH \rightarrow CHOH \rightarrow CHO \rightarrow CO$; (III) $CH_3OH \rightarrow CH_2OH \rightarrow CHOH \rightarrow COH \rightarrow CO$.

IM6 is another binding geometry of methanol on Pt$_3$ cluster, where an H atom in methyl interacts with a Pt atom. It is a necessary configuration for the C-H bond scission though it is energetically less favorable by 10.83 kcal mol⁻¹ than IM1 discussed above. Such metastable configuration was also found to be real for methanol adsorption on the Pt (111) surface [38]. We locate a transition state structure connecting IM1 and IM6, denoted as TS$_{1-6}$. The relaxed rotational barrier from IM1 to IM6 is calculated to be

10.84 kcal mol⁻¹. Once IM6 is formed, the C-H bond scission can occur via TS$_{6-7}$ with a barrier of 3.56 kcal mol⁻¹ to form IM7, a common intermediate along the three branches.

As is shown in Fig. 3, the first branch proceeds according to the pathway IM7$\rightarrow$TS$_{7-8}$$\rightarrow$IM8$\rightarrow$TS$_{8-9}$$\rightarrow$IM9$\rightarrow$TS$_{9-10}$$\rightarrow$IM10 after the initial C-H bond cleavage. TS$_{7-8}$, TS$_{8-9}$, and TS$_{9-10}$ correspond to the transition states dissociating the O-H bond, the second and third C-H bonds, respectively. The calculated barriers for these three elementary steps are 8.04, 12.99, and 12.79 kcal mol⁻¹. Note that TS$_{7-8}$, which corresponds to the transition state breaking the O-H bond, involves two Pt atoms. It is found that all the intermediates and transition states involved along this branch are located to lie below the reaction entrance. Compared to the other two branches to be discussed below along the C-H bond scission pathway, this branch is found to be energetically most favorable, which proceeds via intermediates CH_2OH, CH_2O, and CHO.

The other two branches II and III proceed according to the pathway of IM7$\rightarrow$TS$_{7-11}$$\rightarrow$IM11$\rightarrow$TS$_{11-12}$$\rightarrow$IM12$\rightarrow$TS$_{12-13}$$\rightarrow$IM13 and the pathway of IM7$\rightarrow$TS$_{7-11}$$\rightarrow$IM11$\rightarrow$TS$_{11-14}$$\rightarrow$IM14$\rightarrow$TS$_{14-5}$$\rightarrow$IM5, respectively. Note that TS$_{7-11}$, which corresponds to the transition state activating the second C-H bond, also involves two Pt atoms. As seen in Fig. 3, TS$_{7-11}$, TS$_{11-14}$, and TS$_{14-5}$ are located to lie much above branch I, and so branches II and III are not expected to be competitive with branch I.

It is noted that the overall reaction for the methanol dehydrogenation to CO was highly exothermic. IM10, where four H atom in the methanol molecule have all transferred onto Pt$_3$ and adsorbed CO has been formed, is located to lie below the reaction entrance by 18.65 kcal mol⁻¹. As shown in Fig. 4, all three branches along the initial C-H bond scission require an ensemble comprised of 2 Pt atoms to accommodate the intermediates and transition states.

Fig. 4 Optimized geometries of intermediates and transition states involved in the methanol dehydrogenation reaction starting from C-H bond scission over Pt₃ cluster. The blue, gray, red, and white balls denote Pt, C, O and H atoms, respectively. The distances are in Å
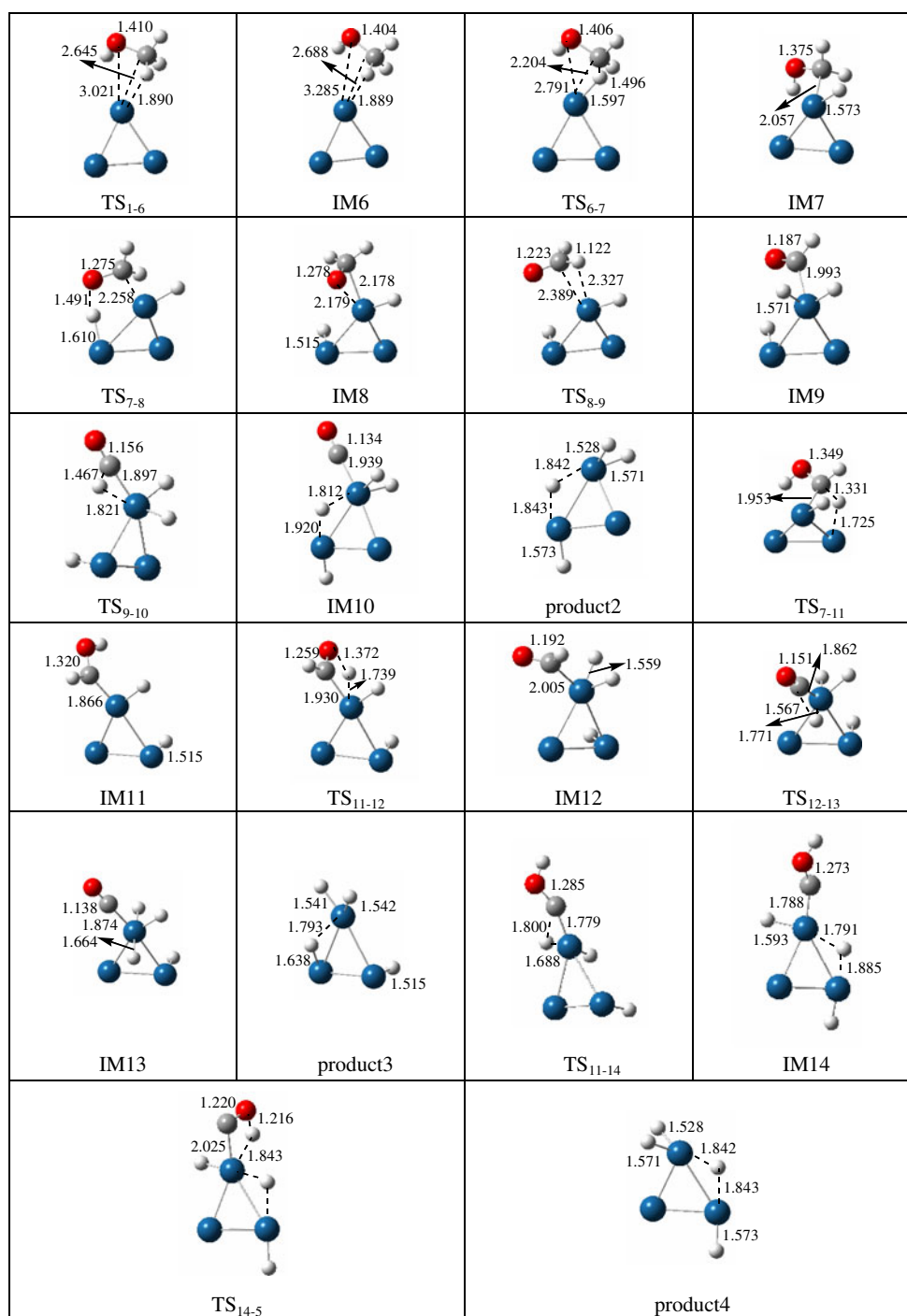
Comparing Fig. 3 with Fig. 1, we have seen that the most favorable C-H bond scission pathway (branch I) also overmatches the O-H bond scission pathway. Thus we propose that the methanol oxidation on pure Pt clusters may preferentially proceed according to the C-H scission pathway via CH_2OH, CH_2O, and CHO intermediates. This is in agreement with the result on Pt(111) presented by Greeley and Mavrikakis [39].

From the results above, it is clear that the methanol decomposition along the C-H scission pathway over Pt₃ involves an ensemble with two Pt atoms. In addition, it is noted that the overall reaction for the methanol dehydrogenation to CO was highly exothermic. The energy needed for CO dissociation from IM10 is calculated to be as high as 30.27 kcal mol⁻¹, suggesting that the population of CO on Pt catalysts is large. This is

Fig. 5 Potential energy profile of methanol dehydrogenation starting from O–H bond scission over Au$_2$Pt cluster. The energies include zero-point energy corrections
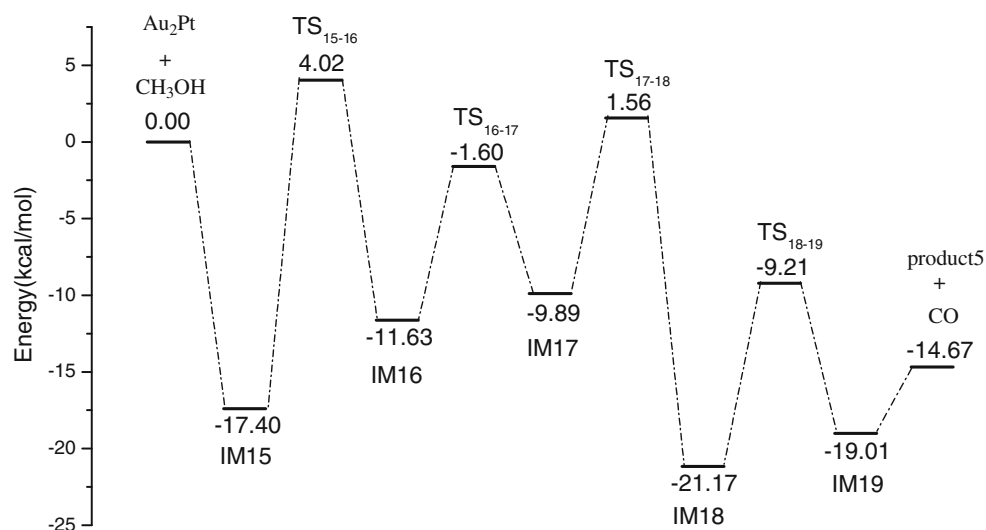
consistent with the well-known fact that Pt catalysts are very easy to be poisoned by CO [58].

O–H bond scission pathway over PtAu$_2$

For the methanol oxidation over PtAu$_2$, two possible situations have been taken into account: the reaction occurs on Pt and Au sites, respectively. The calculated results indicate that the reaction on Pt site is energetically more favorable than on Au site, implying that the Pt sites in PtAu bimetallic nanoparticles are the catalytically active center. For example, for the reaction of the O-H bond scission on Au site of PtAu$_2$ cluster, the calculated barrier is 43.91 kcal mol^{-1},

which is higher by 22.49 kcal mol^{-1} than that which occurs on Pt site. For simplification, here we only give the results for the reaction occurring on Pt active center. Figure 5 shows the energy diagram for the methanol decomposition on PtAu$_2$ cluster starting from O–H bond scission pathway. Figure 6 gathers the geometries of intermediates (IM15-IM19) and transition states (TS$_{15-16}$, TS$_{16-17}$, and Ts$_{18-19}$) involved along this pathway.

We find that the mechanism details for the reaction over binary PtAu$_2$ cluster are very similar to that over monometal Pt$_3$ cluster. The reaction starts from the initial intermediate IM15, where the methanol molecule binds to the on-top site of the Pt site through its O atom. Through four sequential dehydrogenation steps with barriers of 21.42,

Fig. 6 Optimized geometries of intermediates and transition states involved in the methanol dehydrogenation reaction starting from O–H bond scission over Au$_2$Pt cluster. The blue, yellow, gray, red, and white balls denote Pt, Au, C, O and H atoms, respectively. The distances are in Å
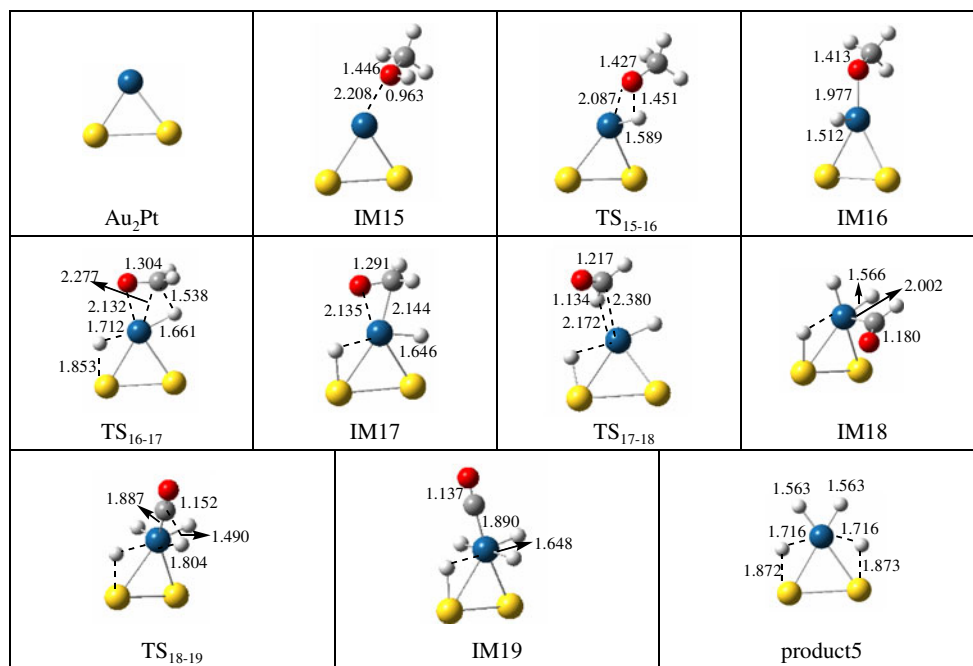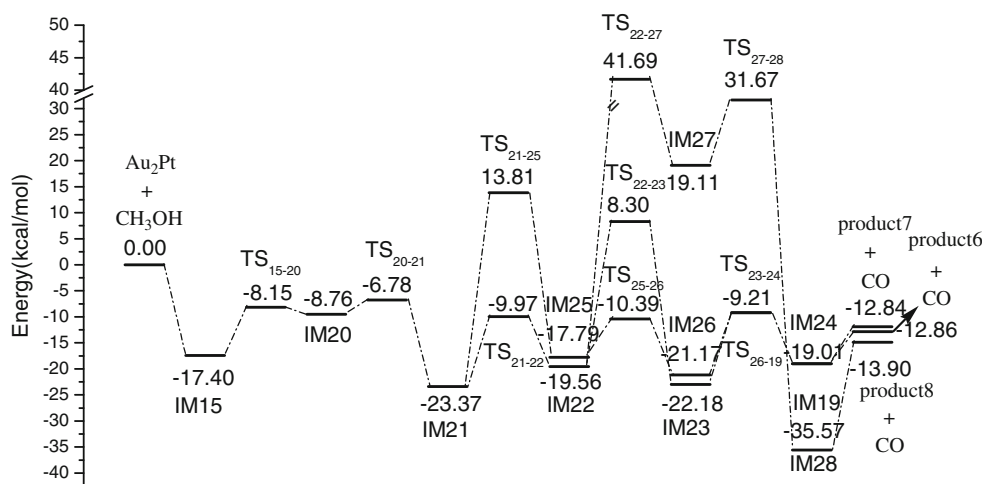
Fig. 7 Potential energy profile of methanol dehydrogenation starting from C-H bond scission over Au$_2$Pt cluster. The energies include zero-point energy corrections

10.03, 11.45, and 11.96 kcal mol^{-1}, the methanol is finally oxidized into CO molecule. The rate-determining step is still the initial O-H bond cleavage, which is lower by 3.48 kcal mol^{-1} than that on the Pt$_3$ cluster, implying that PtAu bimetallic catalysts may facilitate the reaction pathway that starts from the O-H bond scission. The overall reaction from the binding of methanol to the formation of CO was calculated to be exothermic by 1.61 kcal mol^{-1}.

Comparing Fig. 5 with Fig. 1, we observe a remarkable point that the final CO dissociation from PtAu$_2$ cluster needs only an energy of 4.34 kcal mol^{-1}, which is much lower than that (30.27 kcal mol^{-1}) from Pt$_3$ cluster. This indicates that CO binds more weakly on PtAu$_2$ cluster than on Pt$_3$ cluster. In other words, the bimetallic cluster can reduce the extent of CO poisoning [18], which is in agreement with the observed fact modifying Pt with Au can obviously speed up the removal of CO poisonous species to maintain the activity of reaction cycle [59]. From Fig. 6, we note that all four elementary step activating O-H and C-H bonds occur on the Pt site. This fact implies that Pt atoms in PtAu bimetallic catalysts are the main dehydrogenation sites and the role of Au atoms is to speed up the removal of CO.

As is to be discussed in the following section, the O-H bond scission pathway over PtAu$_2$ is also relatively more favorable than the C-H bond scission pathway. This clearly differs from the reaction over Pt$_3$ cluster, where the reaction preferentially proceeds along the C-H scission pathway.

## C–H bond scission pathway over PtAu$_2$

Similar to the case over Pt$_3$ along the C-H bond scission pathway, we further studied the methanol dehydrogenation reaction along three branches shown in Scheme 1. It is found that in all situations the reaction prefers to occur on the Pt site to the Au site, implying that Pt sites in the bimetallic nanoparticles act as the

catalytically active centers (dehydrogenation sites) again. Figures 7 and 8 show the calculated energy diagrams and optimized geometries of intermediates and transition states, respectively.

IM20, where one of the C-H bonds in the methanol molecule weakly binds to the Pt atom, is a necessary intermediate to carry out the initial C-H bond scission. It arises from IM15 via TS$_{15-20}$ with a barrier of 9.25 kcal mol^{-1}. Once IM20 is formed, it is easily converted into IM21 by breaking the first C-H bond with a barrier of only 1.98 kcal mol^{-1}. As shown in Fig. 8, after IM21 the reaction evolves into different branches. Similar to the process over Pt$_3$, we have seen that branch I (CH$_3$OH → CH$_2$OH → HCOH → CHO → CO, i.e., the pathway IM21→TS$_{21-22}$→ IM22→TS$_{22-23}$→IM23→TS$_{23-24}$→IM24 in Fig. 8) is energetically much more favorable than branch II (CH$_3$OH → CH$_2$OH → CH$_2$O → CHO → CO, i.e., the pathway IM21→TS$_{21-25}$→IM25→TS$_{25-26}$→IM26→TS$_{26-19}$→ IM19 in Fig. 8) and branch III (CH$_3$OH → CH$_2$OH → HCOH → COH → CO, i.e. IM21→TS$_{21-22}$→IM22→ TS$_{22-27}$→IM27→TS$_{27-28}$→IM28 in Fig. 8). The rate-determining step of branch I is the formation of TS$_{22-23}$ with a barrier of 27.86 kcal mol^{-1}, while those of branches II and III correspond to the formations of transition states TS$_{21-25}$ and TS$_{22-27}$ with barriers of 37.18 and 61.25 kcal mol^{-1}, respectively. These results suggest that species CH$_2$OH, HCOH, and CHO involved in branch I might be the most possible intermediates involved during the methanol dehydrogenation reaction if the reaction proceeds according to the usual CO pathway.

From the discussion above, it is clear that the methanol decomposition on Pt$_3$ cluster dominantly proceeds along the initial C-H bond scission pathway, however, it alters to the O-H bond scission pathway over PtAu$_2$. For the former, the reaction requires an ensemble composed of two Pt atoms; while in the situation of the latter, the single Pt atom in PtAu$_2$ cluster can act as the catalytically active center. In

Fig. 8 Optimized geometries of intermediates and transition states involved in the methanol dehydrogenation reaction starting from C-H bond scission over Au₂Pt cluster. The blue, yellow, gray, red, and white balls denote Pt, Au, C, O and H atoms, respectively. The distances are in Å
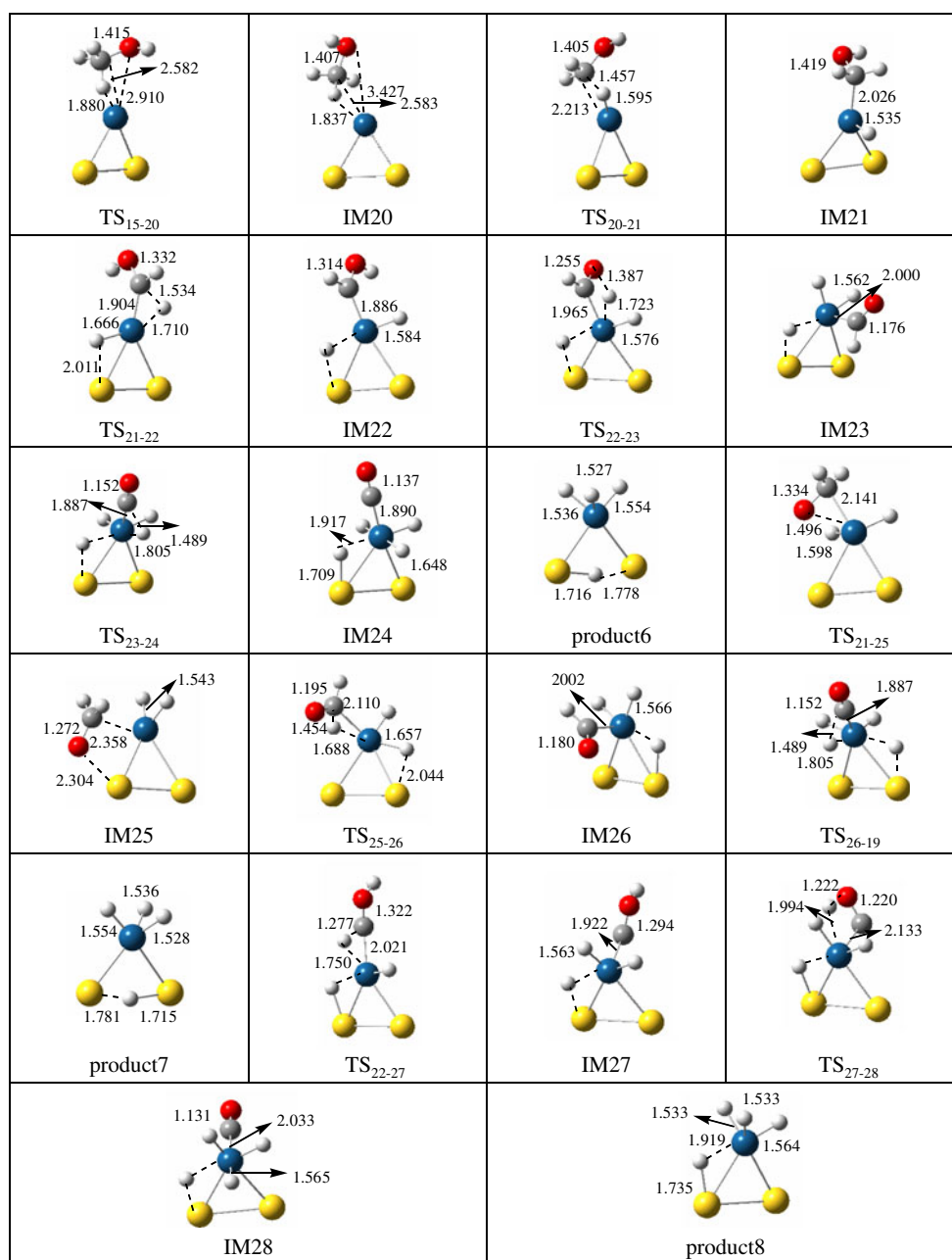
particular, we find that the CO dissociation from PtAu₂ is much more favorable than from Pt₃ cluster.

It should be noted that our calculations were carried out in vacuum using the isolated gas-phase cluster models without considering the effect of solvent on the reactivity. However, we emphasize that gas-phase clusters are valuable model systems for investigating the reaction taking place on catalytic surfaces [48]. A study of the reactions of free clusters can provide useful information for understanding the mechanisms involved in the realistic and complicated catalytic systems. In the present work, our main aim is to present a comparative study of the relative activation of Pt₃ and PtAu₂ clusters

toward the methanol dehydrogenation, which is the first step for understanding the enhanced catalytic activity of bimetallic PtAu catalysts. On the other hand, it is expected that the solvent effect should have similar influence on the reactivity of two clusters, and thus would not change the main conclusions drawn out from our present gas calculations.

Conclusions

In summary, we have performed a comparative theoretical study for methanol dehydrogenation over Pt₃ and PtAu₂

clusters. The following conclusions can be drawn out from the present calculations:

i From an energetic point of view, the methanol dehydrogenation promoted by Pt_3 cluster preferentially proceeds along the initial C-H bond scission pathway, while the optimal one for the $PtAu_2$-promoted reaction alters to the initial O-H bond scission pathway.

ii The barrier of the rate-determining step for Pt_3-promoted reaction is calculated to be 12.99 kcal mol^{-1}, which is lower than that (21.42 kcal mol^{-1}) for $PtAu_2$-promoted reaction. However, it is found that the complete dehydrogenation product of methanol, CO, can much more easily dissociate from $PtAu_2$ cluster than from Pt_3 cluster.

iii The optimal pathway starting from the C-H bond scission over Pt_3 cluster involves an ensemble composed of two Pt atoms, in contrast, the single Pt atom in $PtAu_2$ can fulfill the methanol dehydrogenation to CO along the energetically favorable O-H bond scission pathway.

These conclusions may be enlightening to understand the detailed mechanism and improved catalytic activity of PtAu bimetallic catalysts toward methanol oxidation and to further design efficient catalysts used in DMFC.

References

1. Parsons R, Vandernoot T (1988) The oxidation of small organic molecules A survey of recent fuel cell related research. J Electroanal Chem 257:9–45
2. Reddington E, Sapienza A, Gurau B, Viswanathan R, Sarangapani S, Smotkin ES, Mallouk TE (1998) Combinatorial electrochemistry: a highly parallel, optical screening method for discovery of better electrocatalysts. Science 280:1735–1737
3. Petrii OA (2008) Pt–Ru electrocatalysts for fuel cells: a representative review. J Solid State Electrochem 12:609–642
4. Sun YP, Xing L, Scott K (2010) Analysis of the kinetics of methanol oxidation in a porous Pt–Ru anode. J Power Sources 195:1–10
5. Luo J, Njoki PN, Lin Y, Mott D, Wang LY, Zhong CJ (2006) Characterization of Carbon-Supported AuPt Nanoparticles for Electrocatalytic Methanol Oxidation Reaction. Langmuir 22:2892–2898
6. Luo J, Maye MM, Kariuki NN, Wang LY, Njoki PN, Lin Y, Schadt M, Naslund HR, Zhong CJ (2005) Electrocatalytic oxidation of methanol: carbon-supported gold–platinum nanoparticle catalysts prepared by two-phase protocol. Catal Today 99:291–297
7. Xu CX, Wang RY, Chen MW, Zhang Y, Ding Y (2010) Dealloying to nanoporous Au/Pt alloys and their structure sensitive electrocatalytic properties. Phys Chem Chem Phys 12:239–246
8. Jusys Z, Kaiser J, Behm RJ (2002) Composition and activity of high surface area PtRu catalysts towards adsorbed CO and methanol electrooxidation-A DEMS study. Electrochim Acta 47:3693–3706
9. Sinfelt JH (1983) Bimetallic Catalysts: DiscoVeries, Concepts, and Applications: Exxon Monograph. Wiley, New York
10. Sinfelt JH (1987) Structure of Bimetallic Clusters. Acc Chem Res 20:134–139
11. Ferrando R, Jellinek J, Johnston RL (2008) Nanoalloys: From Theory to Applications of Alloy Clusters and Nanoparticles. Chem Rev 108:845–910
12. Hernández-Fernández P, Montiel M, Ocón P, Fierro JLG, Wang H, Abruña HD, Rojas S (2010) Effect of Co in the efficiency of the methanol electrooxidation reaction on carbon supported Pt. J Power Sources 195:7959–7967
13. Morante-Catacora TY, Ishikawa Y, Cabrera CR (2008) Sequential electrodeposition of Mo at Pt and PtRu methanol oxidation catalyst particles on HOPG surfaces. J Electroanal Chem 621:103–112
14. Neto AO, Dias RR, Tusi M, Linardi M, Spinacé EV (2007) Electro-oxidation of methanol and ethanol using PtRu/C, PtSn/C and PtSnRu/C electrocatalysts prepared by an alcohol-reduction process. J Power Sources 166:87–91
15. Yi QF, Zhang JJ, Chen AC, Liu XP, Xu GR, Zhou ZH (2008) Activity of a novel titanium-supported bimetallic PtSn/Ti electrode for electrocatalytic oxidation of formic acid and methanol. J Appl Electrochem 38:695–701
16. Balakrishnan K, Sachdev A, Schwank J (1990) Chemisorption and FTIR study of bimetallic Pt–-Au/SiO2 catalysts. J Catal 121:441–445
17. Shen JY, Hill JM, Watwe RM, Podkolzin SG, Dumesic JA (1999) Ethylene adsorption on Pt/Au/SiO$_2$ catalysts. Catal Lett 60:1–9
18. Tang W, Jayaraman S, Jaramillo TF, Stucky GD, McFarland EW (2009) Electrocatalytic activity of gold-platinum clusters for low temperature fuel cell applications. J Phys Chem C 113:5014–5024
19. Selvarani G, Vinod Selvaganesh S, Krishnamurthy S, Kiruthika GVM, Sridhar P, Pitchumani S, Shukla AK (2009) A methanol-tolerant carbon-supported Pt-Au alloy cathode catalyst for direct methanol fuel cells and its evaluation by DFT. J Phys Chem C 113:7461–7468
20. Guo X, Guo DJ, Qiu XP, Chen LQ, Zhu WT (2008) A simple one-step preparation of high utilization AuPt nanoparticles supported on MWCNTs for methanol oxidation in alkaline medium. Electrochem Commun 10:1748–1751
21. Guo X, Guo DJ, Chen LQ, Zhu WT, Qiu XP (2008) A simple one-step preparation of high utilization AuPt nanoparticles supported on MWCNTs for methanol oxidation in alkaline medium. Electrochem Commun 10:1748–1751
22. Hu YJ, Zhang H, Wu P, Zhang H, Zhou B, Cai CX (2011) Bimetallic Pt–Au nanocatalysts electrochemically deposited on graphene and their electrocatalytic characteristics towards oxygen reduction and methanol oxidation. Phys Chem Chem Phys 13:4083–4094
23. Silva DF, Geraldes AN, Cardoso EZ, Tusi MM, Linardi M, Spinacé EV, Neto AO (2011) Preparation of PtAu/C and PtAuBi/C electrocatalysts using electron beam irradiation for methanol and ethanol electro-oxidation in alkaline medium. Int J Electrochem Sci 6:3594–3606
24. Batista EA, Malpass GRP, Motheo AJ, Iwasita T (2003) New insight into the pathways of methanol oxidation. Electrochem Commun 5:843–846
25. Cao D, Lu GQ, Wieckowski A, Wasileski SA, Neurock M (2005) Mechanisms of methanol decomposition on platinum: a combined experimental and *ab initio* approach. J Phys Chem B 109:11622–11633
26. Hoster H, Iwasita T, Baumgartner H, Vielstich W (2001) Pt-Ru model catalysts for anodic methanol oxidation: influence of structure and composition on the reactivity. Phys Chem Chem Phys 3:337–246

27. Housmans THM, Koper MTM (2003) Methanol oxidation on stepped Pt[n(111)×(110)] electrodes: a chronoamperometric study. J Phys Chem B 107:8557–8567

28. Housmans THM, Wonders AH, Koper MTM (2006) Structure sensitivity of methanol electrooxidation pathways on platinum: an on-line electrochemical mass spectrometry study. J Phys Chem B 110:10021–10031

29. Iwasita T, Hoster H, John-Anacker A, Lin WF, Vielstich W (2000) Methanol oxidation on PtRu electrodes. Influence of surface structure and Pt-Ru atom distribution. Langmuir 16:522–529

30. Iwasita T (2002) Electrocatalysis of methanol oxidation. Electrochim Acta 48:289–289

31. Iwasita T (2002) Electrocatalysis of methanol oxidation. Electrochim Acta 47:3663–3674

32. Jusys Z, Behm RJ (2001) Methanol oxidation on a carbon-supported Pt Fuel cell catalyst-A kinetic and mechanistic study by differential electrochemical mass spectrometry. J Phys Chem B 105:10874–10883

33. Gasteiger HA, Markovic N, Ross PN, Cairns EJ (1993) Methanol electrooxidation on well-characterized Pt-Ru alloys. J Phys Chem 97:12020–12029

34. Tripkovic AV, Popovic KD, Grgur BN, Blizanac B, Ross PN, Markovic NM (2002) Methanol electrooxidation on supported Pt and PtRu catalysts in acid and alkaline solutions. Electrochim Acta 47:3707–3714

35. Kardash D, Korzeniewski C, Markovic N (2001) Effects of thermal activation on the oxidation pathways of methanol at bulk Pt–Ru alloy electrodes. J Electroanal Chem 500:518–523

36. Davis JL, Barteau MA (1987) Decarbonylation and decomposition pathways of alcohol's on Pd(111). Surf Sci 187:387–406

37. Bagotzky VS, Vassiliev YB, Khazova OA (1977) Generalized scheme of chemisorption, electrooxidation and electroreduction of simple organic compounds on platinum group metals. J Electroanal Chem 81:229–238

38. Greeley J, Mavrikakis M (2002) A First-Principles Study of Methanol Decomposition on Pt(111). J Am Chem Soc 124:7193–7201

39. Greeley J, Mavrikakis M (2004) Competitive Paths for Methanol Decomposition on Pt(111). J Am Chem Soc 126:3910–3919

40. Watanabe T, Ehara M, Kuramoto K, Nakatsuji H (2009) Possible reaction pathway in methanol dehydrogenation on Pt and Ag surfaces/clusters starting from O–H scission: Dipped adcluster model study. Surf Sci 603:641–646

41. Yuan DW, Gong XG, Wu RQ (2008) Decomposition pathways of methanol on the PtAu(111) bimetallic surface: A first-principles study. J Chem Phys 128:064706

42. Maroun F, Ozanam F, Magnussen OM, Behm RJ (2001) The role of atomic ensembles in the reactivity of bimetallic electrocatalysts. Science 293:1811–1814

43. Chen MS, Kumar D, Yi CW, Goodman DW (2005) The Promotional Effect of Gold in Catalysis by Palladium-Gold. Science 310:291–293

44. Tong YY (2005) A coverage-dependent study of Pt spontaneously deposited onto Au and Ru surfaces: direct experimental evidence of the ensemble effect for methanol electro-oxidation on Pt. J Phys Chem B 109:17775–17778

45. Cuesta A (2006) At least three contiguous atoms are necessary for CO formation during methanol electrooxidation on platinum. J Am Chem Soc 128:13332–13333

46. Neurock M, Janik M, Wieckowski A (2009) A first principles comparison of the mechanism and site requirements for the electrocatalytic oxidation of methanol and formic acid over Pt. Faraday Discuss 140:363–378

47. Yuan DW, Gong XG, Wu RQ (2007) Atomic configurations of Pd atoms in PdAu(111) bimetallic surfaces investigated using the first-principles pseudopotential plane wave approach. Phys Rev B 75:085428

48. Fialko EF, Kikhtenko AV, Goncharov VB, Zamaraev KI (1997) Similarities between reactions of methanol with $Mo_xO_y^+$ in the gas phase and over real catalysts. J Phys Chem B 101:5772–5773

49. Wallace WT, Whetten RL (2002) Coadsorption of CO and O_2 on Selected Gold Clusters: Evidence for Efficient Room-Temperature CO_2 Generation. J Am Chem Soc 124:7499–7505

50. Frisch MJ, Trucks GW, Schlegel HB, Scuseria GE, Robb MA, Cheeseman JR, Montgomery JA Jr, Vreven T, Kudin KN, Burant JC, Millam JM, Iyengar SS, Tomasi J, Barone V, Mennucci B, Cossi M, Scalmani G, Rega N, Petersson GA, Nakatsuji H, Hada M, Ehara M, Toyota K, Fukuda R, Hasegawa J, Ishida M, Nakajima T, Honda Y, Kitao O, Nakai H, Klene M, Li X, Knox JE, Hratchian HP, Cross JB, Adamo C, Jaramillo J, Gomperts R, Stratmann RE, Yazyev O, AJ Austin, Cammi R, Pomelli C, Ochterski JW, Ayala PY, Morokuma K, Voth GA, Salvador P, Dannenberg JJ, Zakrzewski VG, Dapprich S, Daniels AD, Strain MC, Farkas O, Malick DK, Rabuck AD, Raghavachari K, Foresman JB, Ortiz JV, Cui Q, Baboul AG, Clifford S, Cioslowski J, Stefanov BB, Liu G, Liashenko A, Piskorz P, Komaromi I, Martin RL, Fox DJ, Keith T, Al- Laham MA, Peng CY, Nanayakkara A, Challacombe M, Gill PMW, Johnson B, Chen W, Wong MW, Gonzalez C, Pople JA (2003) Gaussian03, Revision B.02. Gaussian Inc, Pittsburgh, PA

51. Becke AD (1993) Density-functional thermochemistry. III. The role of exact exchange. J Chem Phys 98:5648–5652

52. Becke AD (1988) Density-functional exchange-energy approximation with correct asymptotic behavior. Phys Rev A 38:3098–3100

53. Lee CT, Yang WT, Parr RG (1988) Development of the Colic-Salvetti correlation-energy formula into a functional of the electron density. Phys Rev B 37:785–789

54. Hay PJ, Wadt WR (1985) *Ab initio* effective core potentials for molecular calculations. Potentials for the transition metal atoms Sc to Hg. J Chem Phys 82:270–283

55. Hay PJ, Wadt WR (1985) *Ab initio* effective core potentials for molecular calculations. Potentials for K to Au including the outermost core orbitals. J Chem Phys 82:299–310

56. Fukui K (1970) A formulation of the reaction coordinate. J Phys Chem 74:4161–4163

57. Perdew JP, Burke K, Ernzerhof M (1996) Generalized Gradient Approximation Made Simple. Phys Rev Lett 77:3865–3868

58. Beden B, Morin MC, Hahn F (1987) "In situ" analysis by infrared reflectance spectroscopy of the adsorbed species resulting from the electrosorption of ethanol on platinum in acid medium. J Electroanal Chem 229:353–366

59. Ren H, Humbert MP, Menning CA, Shu YY, Singh UG, Cheng WC, Chen JG (2010) Inhibition of coking and CO poisoning of Pt catalysts by the formation of Au/Pt bimetallic surfaces. Appl Catal A 375:303–309